A weakly-compressible DNS formalism for turbulent atomization applications

Benjamin Duret, R. Canu, J. Reveillon, F.-X Demoulin

A weakly-compressible DNS formalism for turbulent atomization applications

B. Duret*, R. Canu, J. Reveillon, F.-X. Demoulin
UMR 6614 CORIA, Technopôle du Madrillet, B.P. 12, Avenue de l'Université, 76801 Saint Etienne du Rouvray Cedex, France

Abstract

Compressible or weakly compressible liquid-gas flows occur in many fields such as liquid fuel injection, plunging waves, cavitation, sloshing, drowning damaged nuclear reactor, phase change heat transfer, pipeline of two-phase flows, etc. Most numerical simulations dedicated to the aforementioned applications use an incompressible formalism, which does not take into account the compressibility effects and density variation among each phase. However, compressibility can have a significant effect in a wide range of configuration, from liquid jet injection (cavitation inside an injector) to breaking wave configuration (impact of the entrained air or bubbles). This work aims at providing numerical tools, allowing simulations of two-phase flows covering a large range of Mach number, incorporating surface tension, acoustic/compressible effects, large density ratio, proper jump conditions, viscous effects, at High Reynolds and High Weber number. We propose achieving this challenging task by improving the two-phase flows aspect of the pressure-based method proposed by Huber et al (2015) [Journal of Computational Physics, Volume 302, 2015, Pages 439-468] by combining it with an accurate and conservative interface representation : the Coupled Level Set/VOF interface capturing method. First, a one-dimensional oscillating water column configuration is investigated to perform the validation of this method. Then, a three-dimensional two-phase HIT configuration is studied to demonstrate the behavior and the potential of this method in presence of breakup, coalescence and vaporization processes.

Introduction

Compressible or weakly compressible liquid-gas flows occur in many fields such as liquid fuel injection, plunging waves, cavitation, sloshing, drowning damaged nuclear reactor, phase change heat transfer, pipeline of two-phase flows, etc. Liquid-gas flows has a direct impact on gas emissions (atomization in combustion engines), industrial process efficiency (heat exchanger) or coastal engineering (breaking wave). Most numerical simulations dedicated to the aforementioned applications use an incompressible formalism, which does not take into account the compressibility effects and density variation among each phase. However, compressibility can have a significant effect in a wide range of configuration, from liquid jet injection (cavitation inside an injector) to breaking wave configuration (impact of the entrained air or bubbles). Indeed, vapor production or cavitation inside an injector generate a creation of volume (non-zero divergence of the velocity field) incompatible with the standard incompressible hypothesis used mainly in liquid-gas flows simulations.

The use of a compressible, variable-density solver is also mandatory to describe phase change in complex configurations such as liquid jet injection or breaking waves. Handling phase change in numerous gas inclusion, each possessing their own gas density evolution and thermodynamic pressure, is not straightforward. In our previous works, the phase change description was based on an incompressible solver : first by using a passive scalar to focus on the mixing process [1], then by computing the evaporation rate based on temperature and species equations, allowing to evaluate the velocity jump condition and gas dilatation [2, 3]. The latter formulation is encouraging but is not suitable with the presence of multiple gas inclusions or in a confined environment, since the gas and vapor density remains constant in that formalism.

The main objective of this article is to break a scientific barrier concerning the numerical simulation of compressible liquid-gas flows. Indeed, the majority of accurate numerical methods used in two-phase flows simulation with interface tracking/capturing method can be categorized in two families: incompressible [4] or compressible method [5]. Very different formalism are used to solve the governing equations (Poisson solver versus Riemann solver) and only few collaborations exist between the "incompressible" and the "compressible" communities. The drawback of these methods is their inability to capture accurately and smoothly two-phase flows with a wide evolution of the compressibility effects, from (very) low Mach number to high Mach number.

This issue was solved in the case of single phase flows or reacting flows with the low Mach approach [6], which has been used to represent the expansion/compression of gas and density variations. However, this kind of approach is not straightforward in the context of two-phase flows. The existence of inclusions (bubbles) of gas

*Corresponding author: duret@coria.fr

inside a liquid imposes a complex way to take into account the gas density variation inside each inclusion. Indeed, the thermodynamic pressure difference in each inclusion make the equation difficult to solve with a one-field approach [7]. A solution is to account for the density variation by integrating the incoming fluxes on the boundary of the bubble, or use an extension to take into account the jump of thermodynamics pressure. Nevertheless, gas inclusions and their surface have to be tracked to properly estimate the mean density variation. It means that it will be impossible to simulate realistic large scale configurations with numerous gas inclusions because of the computational cost involved.

In regards to atomization processes, most DNS/LES studies are considered incompressible, despite the fact that the initial injection velocity can be close or higher than the celerity of sound in the gas phase. For instance, in the Engine Combustion network injector called "Spray A" [8], the injection velocity is around $600\ m.s^{-1}$. Pressure waves developing in front of the liquid jet are then likely to be observed (for instance in [8]). Another important topic is the cavitation process inside injectors nozzles, taking into account compressibility will give a new insight into identifying cavitation zones in the liquid phase and understanding the effect of cavitation on the atomization process. This illustrates the need of new and original numerical developments to fully resolve both phases and also acoustic effects.

Some attempts has been made recently to solve these specifics issues : Miller et al. [9] proposed one of the first pressure-based formalism using a Volume Of Fluid (VOF) interface capturing method in OpenFOAM, showing encouraging results on underwater explosions and shock tubes configurations with large density ratio. However, the author admits that mass is not well conserved and jump conditions for variable such as density, viscosity are smeared out over a few cells. Huber et al. [10] used a primitive formulation of the compressible Navier Stokes equations to consider compressible two-phase flows, combined with a pressure-based method similar to the one developed in single phase flow context by Kwatra et al. [11]. Acoustics terms where treated implicitly along with a proper description of surface tension forces. This method has been compared with a standard compressible solver (preconditioned explicit HLLC), showing that better results has been obtained with the pressure-based method on a oscillating bubble configuration (Rayleigh-Plesset theory). Boger et al. [12] performed a similar study by using a pressure-based method to study shock-droplet interaction. However, these methods are coupled with a Level-Set approach, making turbulent atomization difficult to handle (mass loss) and viscous effects are not taken into account.

This work aims at providing numerical tools, allowing simulations of two-phase flows covering a large range of Mach number, incorporating surface tension, acoustic/compressible effects, large density ratio, proper jump conditions, viscous effects, at High Reynolds and High Weber number. We propose achieving this challenging task by improving the two-phase flows aspect of the pressure-based method proposed by Huber et al. [10] and Miller et al. [9] by combining it with an accurate and conservative interface representation : the Coupled Level Set/VOF interface capturing method. The main emphasis of this study is on the computation of Low Mach number configurations but the method can be used as well in shock waves configurations.

In the following part of this work, the constitutive equations and numerical procedures are first described. Then, an oscillating water column configuration is used to illustrate the accuracy and robustness of the compressible method. Finally, a HIT configuration is presented to introduce the implementation of phase change in compressible turbulent two-phase flows.

Governing Equations

The joint LS/VOF method is coupled with a projection method to carry out the Direct Numerical Simulations of compressible Navier-Stokes equations :

$$\begin{cases} \frac{\partial \rho}{\partial t} + \vec{\nabla}.\left(\rho \vec{u}\right) = 0 \\ \frac{\partial \rho \vec{u}}{\partial t} + \vec{\nabla}.\left(\rho \vec{u} \otimes \vec{u}\right) = -\vec{\nabla} P + \vec{\nabla}.\left(2\mu\epsilon + \left(\zeta - \frac{2}{3}\mu\right)\vec{\nabla}.\vec{u}\bar{I}\right) + \rho \vec{f} \end{cases} \tag{1}$$

with ρ, the density ; $\vec{u}$, the velocity ; P, the pressure ; μ, the dynamic viscosity ; $\epsilon = \frac{1}{2}\left(\vec{\nabla}\vec{u} + \vec{\nabla}\vec{u}^t\right)$, the strain rate tensor ; ζ, the second viscosity ; $\vec{f}$, the force of volume by unit of mass and $\bar{I}$, the identity matrix. Here, both liquid and gas are considered as compressible. On the interface, surface tension is taken into account by considering the variables jump across the interface liquid/gas :

$$\left[\vec{n}.\left(P\bar{I} - \bar{\tau}\right).\vec{n}\right] = \sigma\kappa \tag{2}$$

with σ, the surface tension ; κ, the total curvature ; $\vec{n}$, the normal to the interface ; $\bar{\tau}$, the viscous strain tensor defined by $\bar{\tau} = 2\mu\epsilon + \left(\zeta - \frac{2}{3}\mu\right)\vec{\nabla}.\vec{u}\bar{I}$ and the convention $[A] = A_l - A_g$ for the variables jump across the interface.

Eq.1 is closed by two equations of state (EOS). For the liquid, a Tait equation is used and for the gas, it's a Laplace's law thus considering a perfect gas and an isentropic process.

$$\begin{cases} \rho_g = \left(\frac{P}{C_\gamma}\right)^{\frac{1}{\gamma_g}} \\ \rho_l = \rho_0 \left(\frac{P-P_0}{B} + 1\right)^{\frac{1}{\gamma_l}} \end{cases} \tag{3}$$

The g and l index denote respectively the gas and the liquid ; γ represents the adiabatic index ; P_0, a reference pressure ; ρ_0, a reference density ; C_γ, a constant depending on the initial condition of the perfect gas studied and B, a constant depending on the bulk modulus of the considered fluid.

Numerical and/or Experimental Methods

Interface capturing method

The interface is solved using a CLSVOF algorithm. This method allows an accurate representation of the interface with the Level Set function and the mass conservation with the VOF method. The general algorithm can be found in the literature [4]. However, contrary to the algorithm of Menard et al. [4], an additional term due to compressibility has to be taken into account in the liquid volume fraction equation. The new formulation of this equation is :

$$\frac{\partial \alpha_l}{\partial t} + \vec{\nabla}.\left(\alpha_l \vec{u}\right) = \alpha_l \left(1 - \alpha_l\right) D + \alpha_l \vec{\nabla}.\vec{u} \tag{4}$$

with α_l, the liquid volume fraction and D, a term representing the fluid compressibility and defined by $D = \frac{1}{\rho_g}\frac{D\rho_g}{Dt} - \frac{1}{\rho_l}\frac{D\rho_l}{Dt}$. The $\frac{D}{Dt}$ is the material derivative. Eq.4 is derived from the continuity equation of Eq.1 by considering $\rho = \alpha_l\rho_l + \alpha_g\rho_g$ and $\alpha_g = 1 - \alpha_l$. Contrary to most of the codes using the CLSVOF framework, the pressure P and the densities ρ_l and ρ_g are local variables. In the incompressible CLSVOF algorithm, the liquid volume fraction and Level Set transport equations have the same formulation and are split in the three space directions.

Then, a final equation couples the three directions. To be coherent with the Level Set equation that has no additional term in compressible formulation, the compressibility term D of Eq.4 is only added in the final equation.

All the geometrical informations of the interface are obtained with the Level Set function ϕ. The curvature κ is calculated by $\kappa = \vec{\nabla}.\vec{n}$ with $\vec{n} = \vec{\nabla}\phi/|\vec{\nabla}\phi|$, the normal to the interface.

Projection method

Then, to compute velocity and pressure, the momentum equation of Eq.1 is solved using a projection method adapted to compressible. This method allows to decouple velocity and pressure. An intermediate velocity is first calculated without the pressure term $-\vec{\nabla}P$ and the surface tension term :

$$\vec{u}^* = \underbrace{\frac{\rho^n\vec{u}^n}{\rho^*} - \Delta t\frac{\vec{\nabla}.\left(\left(\rho\vec{u}\right)^n \otimes \vec{u}^n\right)}{\rho^*}}_{\text{I}} + \underbrace{\Delta t\frac{\vec{\nabla}.\left(2\mu\epsilon - \frac{2}{3}\mu\vec{\nabla}.\vec{u}^n\bar{I}\right)}{\rho^*}}_{\text{II}} + \Delta t\vec{f} \tag{5}$$

ρ^* corresponds to the density calculated with $\rho = \alpha_l\rho_l + \alpha_g\rho_g$ but with the new value of α_l obtained after the interface resolution. The viscous term II is solved with a Sussman method that can be found in Sussman et al. [13]. This method takes into account directly the viscous tensor jump across the interface. It was originally developed in a incompressible formalism, so the term $(-\frac{2}{3}\mu\vec{\nabla}.\vec{u}\bar{I})$ was added in this algorithm. The second viscosity ζ is neglected in this work. Regarding the convection term I, the method of Vaudor et al. [14] has been used ensuring consistent mass and momentum flux computation. The mesh is an eulerian staggered grid so the

velocity is computed on the faces of the cells and the other variables (pressure, density, liquid volume fraction, ...) are computed in the center of the cells. This method initially proposed by Rudman [15] consists in calculating the mass flux $\rho\vec{u}$ in the center of the cell by using the continuity equation. The mass flux has to be known in the center of the cell in order to have a second order centered scheme for the divergence operator. A detailed explanation of the algorithm can be found in [14].

Then, the momentum equation is discretised in the following way by using the intermediate velocity obtained previously.

$$\vec{u}^{n+1} = \vec{u}^{*} - \Delta t \frac{\vec{\nabla} P}{\rho^{*}} \tag{6}$$

By applying the divergence operator to Eq.6, an Helmholtz equation for the pressure is obtained (Eq.7). Contrary to the projection method used in incompressible solvers, the divergence of the velocity is no longer zero.

$$-\vec{\nabla}.\left(\frac{\vec{\nabla} P^{n+1}}{\rho^{*}}\right) + \left(\frac{\alpha_l}{\rho_l c_l^2 \Delta t^2} + \frac{\alpha_g}{\rho_g c_g^2 \Delta t^2}\right) P^{n+1} = \left(\frac{\alpha_l}{\rho_l c_l^2 \Delta t^2} + \frac{\alpha_g}{\rho_g c_g^2 \Delta t^2}\right) \left(P^n - \Delta t \vec{u}.\vec{\nabla} P^n\right) - \frac{\vec{\nabla}.\vec{u}^{*}}{\Delta t} \tag{7}$$

with c_l and c_g, respectively the sound speed for liquid and gas. The $\vec{\nabla}.\vec{u}^{*}$ term is solved with a second order centered scheme and $\vec{u}.\vec{\nabla} P$, with a fifth order WENO scheme. A Ghost Fluid method is used to apply the pressure jump due to surface tension forces [4]. The final velocity is computed by Eq.6 using a second order centered scheme for the pressure gradient. A second order Runge Kutta scheme have been used for temporal integration. Finally, the density and sound speed for liquid and gas and the total density are updated with the EOS Eq.3. The compressibility term D used in Eq.4 is solved to be coherent with the pressure term :

$$D^{n+1} = \left(\frac{1}{\rho_g c_g^2} - \frac{1}{\rho_l c_l^2}\right) \left(\frac{P^{n+1} - P^n}{\Delta t} + \vec{u}.\vec{\nabla} P\right) \tag{8}$$

Concerning the time step calculation, a CFL condition similar to the one used by Kang et al. [16] is used. Thanks to the implicit resolution of the acoustics terms in the pressure equation, the CFL condition is the same used for incompressible two-phase flows DNS. Consequently, the time step is larger than the one obtained with an acoustic CFL based on the sound speed.

Validation

Oscillating water column configuration

In order to validate the code, an oscillating water column test case has been realized (Figure 1). It consists in the oscillation of a water column between two air columns due to an initial pressure gradient. The liquid compresses a first air column and then, when the pressure in this column exceeds the liquid inertia, the air pushes the water column toward the second air column and so on. This test case can be seen as a Rayleigh-Plesset test case, representing the oscillation of an air bubble inside liquid, but in a 1D cartesian geometry. This test case has been studied previously in some works [7, 17, 18] but by imposing an initial velocity to the liquid column instead of a pressure gradient. However, no reference solution has been developed to compare with numerical results. A theoretical solution can be derived by using mass and momentum conservation and by considering the liquid incompressible. The time evolution of the liquid gas interface is obtained with the following equation :

$$\frac{d^2 R}{dt^2} = \frac{P|_{R_1} - P|_{R_2}}{\rho_l L} \tag{9}$$

$$u = \frac{dR}{dt} \tag{10}$$

with ρ_l, the liquid density ; R_1, the position of the first interface gas-liquid ; R_2, the position of the second interface and $L = R_2 - R_1 = cst$, the liquid length. The pressures in R_1 and R_2 are obtained with the ideal gas

equation of state. Then, the velocity is calculated with Eq.10. No analytical solution was found but a reference solution can be easily computed. It is worth mentioning that the reference solution is considering no pressure fluctuation (Incompressible hypothesis), which is not the case of the numerical method presented here. Consequently, slight differences should be observed on the results when comparing both approaches.

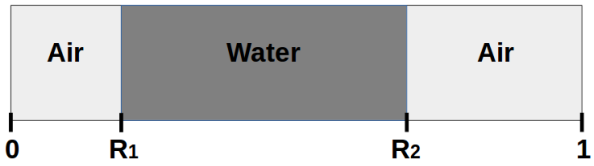

Figure 1. Oscillating Water Column test case

The initial values for density and pressure are referenced in Table 1. The pressure in the first air column is twice the pressure in the second air column and it follows a linear profile in the water column. The water column is located between $R_1 = 0.1\ m$ and $R_2 = 0.8\ m$ and the total domain measures $1\ m$. For the Tait equation in Eq.3, the parameters used are $B = 3.31 \times 10^8\ Pa$, $P_0 = 10^5\ Pa$ and $\rho_0 = 1000\ kg.m^{-3}$.

Air	Water	Air
$0 \leq x \leq R_1$	$R_1 \leq x \leq R_2$	$R_2 \leq x \leq 1$
$\gamma_g = 1.4$	$\gamma_l = 7$	$\gamma_g = 1.4$
$\rho_L = 1.169\ kg.m^{-3}$	$\rho = 1000\ kg.m^{-3}$	$\rho_R = 0.5845\ kg.m^{-3}$
$P_L = 10^5\ Pa$	$P = \frac{P_R - P_L}{R_2 - R_1}x + \frac{P_L R_2 - P_R R_1}{R_2 - R_1}$	$P_R = 5 \times 10^4\ Pa$

Table 1. Initial conditions for the oscillating water column test case. The L and R indexes mean respectively left and right.

For this configuration, the Mach number reaches a maximum value of $M_a = 4.45 \times 10^{-3}$. All the boundary conditions are considered as symmetric.

The Figure 2 compares the evolution in function of time of the velocity of the liquid for different mesh size to the incompressible reference solution. As expected, the velocity oscillates ; initially, the liquid accelerates in the positive x direction due to the pressure gradient until the moment when the pressure is the same in all the domain. Then, the liquid decelerates because the pressure is higher in the second air column, but its velocity is still positive owing to its inertia. Finally, there is again an acceleration followed by a deceleration for the same reasons but in the opposite x direction, hence the negative value of velocity. A mesh convergence is observed in this graph. A $CFL = 0.1$ is performed here ; however, this CFL condition is based on the convective speed (similar to the one used by Kwatra et al. [11] and Huber et al. [10]). The corresponding time step is about 100 times greater than the one obtained from the CFL condition based on the sound speed.

Regarding the mass conservation, a better accuracy is obtained by refining the mesh and the relative error is less than 0.1% for meshes with more than 256 cells (Figure 4).

By using a $CFL = 0.01$ condition, namely a time step about 10 times greater than the one obtained with the acoustic CFL, a convergence is also observed for velocity (Figure 3). The curve is closer to the reference solution but with a slight delay in terms of frequency. Concerning the mass conservation, for a 512 cells mesh, the error obtained is around 0.005% showing minor difference between both CFL. The relative errors for the different meshes are shown in Table 2 for the first maximum for the velocity and for the frequency calculated between the two first maximum of velocity. In all cases, the relative error decreases by refining the mesh, illustrating the method accuracy and convergence.

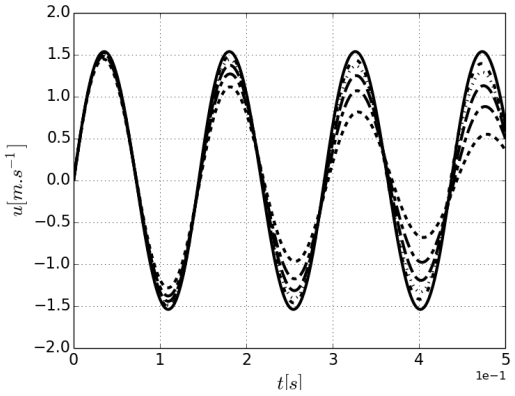

Figure 2. Evolution of the velocity in function of time for different meshes, CFL=0.1 and Runge Kutta 2 scheme.- - - 32 cells,– – – 64 cells, – – – 128 cells, · · · 256 cells, - - - 512 cells. The solid line is the reference solution.

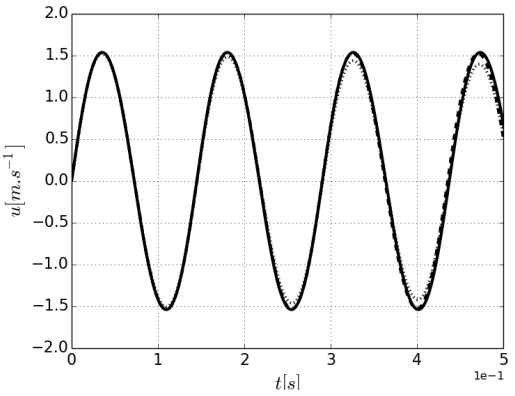

Figure 3. Evolution of the velocity in function of time for 512 cells and Runge Kutta 2 scheme.- - - CFL=0.01, · · · CFL=0.1. The solid line is the reference solution.

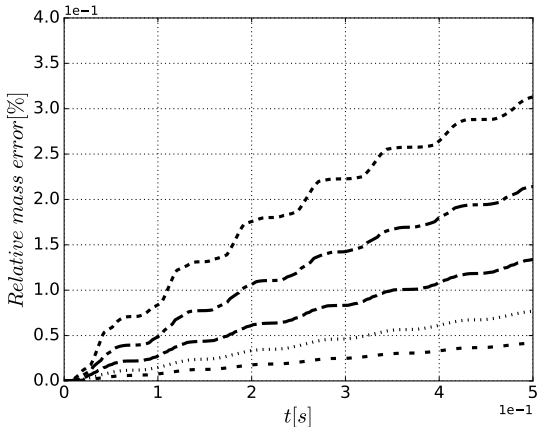

Figure 4. Relative mass of liquid error in function of time for different meshes, CFL=0.1 and Runge Kutta 2 scheme.- - - 32 cells,– – – 64 cells, – – – 128 cells, · · · 256 cells, - - - 512 cells

Nx	32	64	128	256	512
Amplitude Error	5.82	3.66	2.19	1.30	0.49
Frequency Error	1.49	0.87	0.65	0.43	0.35

Table 2. Relative error (%) for a Runge Kutta 2 temporal scheme and CFL=0.1.

HIT configuration with phase change

Governing Equations

In this configuration, phase change is considered. So, mass source terms have to be added both in the liquid volume fraction equation (Eq.4) and the pressure equation (Eq.7). The new formulation of these two equations is the following :

$$\frac{\partial \alpha_l}{\partial t} + \vec{\nabla}.\left(\alpha_l \vec{u}\right) = \alpha_l \left(1-\alpha_l\right) D + \alpha_l \vec{\nabla}.\vec{u} - \alpha_l \dot{m}\left(\frac{1}{\rho_l} - \frac{1}{\rho_g}\right) + \frac{\dot{m}}{\rho_l} \tag{11}$$

$$-\vec{\nabla}.\left(\frac{\vec{\nabla}P^{n+1}}{\rho^*}\right)+\left(\frac{\alpha_l}{\rho_l c_l^2\Delta t^2}+\frac{\alpha_g}{\rho_g c_g^2\Delta t^2}\right)P^{n+1}= \left(\frac{\alpha_l}{\rho_l c_l^2\Delta t^2}+\frac{\alpha_g}{\rho_g c_g^2\Delta t^2}\right)\left(P^n-\Delta t\vec{u}.\vec{\nabla}P^n\right)-\frac{\vec{\nabla}.\vec{u}^*}{\Delta t}+\frac{\dot{m}}{\Delta t}\left(\frac{1}{\rho_l}-\frac{1}{\rho_g}\right) \quad (12)$$

with $\dot{m}$, the mass source term in $[kg.m^{-3}.s^{-1}]$. It is negative when there is an evaporation of the liquid. The two terms in the liquid volume fraction equation come from the liquid density equation obtained by splitting the density in $\rho = \alpha_l\rho_l + \alpha_g\rho_g$. Indeed, even if the total mass is conserved, a source term is necessary in the liquid density equation to take into account phase change. The new term in the pressure equation (Eq.12) comes from the divergence of velocity.

Results

For this Homogeneous Isotropic Turbulence (HIT) validation case (Figure 5), the forcing and the physical parameters used in previous work [1] are applied but with a 256^3 mesh and an initial liquid volume fraction $\phi = 10\%$. The initial densities are $\rho_g = 25.0\ kg.m^{-3}$ and $\rho_l = 753.0\ kg.m^{-3}$. The pressure is $P = 9.06\times10^6\ Pa$ and for the Tait equation, the parameters used are $B = 1.038\times10^9\ Pa$, $P_0 = 10^5\ Pa$ and $\rho_0 = 750\ kg.m^{-3}$. The adiabatic index for the liquid is $\gamma_l = 1.215$ and for the gas is $\gamma_g = 1.4$. For the evaporation, $\dot{m} = -1\ kg.cm^{-3}.s^{-1}$ is chosen. This value is only applied in cells containing an interface ; in all other cells, $\dot{m} = 0\ kg.cm^{-3}.s^{-1}$.

Figure 5. Surface representation of the HIT configuration with $\phi = 10\%$.

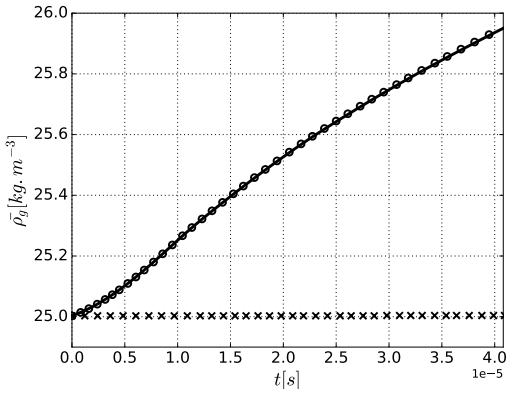

Figure 6. Evolution of the mean gas density in function of time. ∘ : results with evaporation, × : results without evaporation. Solid line : theoretical solution with evaporation.

On Figure 6, the evolution of the mean gas density is represented. As expected, the density remains constant if no evaporation occurs and increases if the mass source term is not zero. Even if $\dot{m}$ is constant, the profile of the density is not linear because the surface quantity is not constant during the process and so, the number of cells containing an interface varies. However, it is still possible to compute the theoretical $\dfrac{\partial\rho_g}{\partial t}$ induced by vaporization if $\dot{m}$ is constant and evaporating cells are identified. Then the time evolution of ρ_g is deduced, as shown on Figure 6. The density profile obtained is very close to the theoretical one showing the capability of the algorithm to represent the evaporation process.

Summary and Conclusions

A pressure based method is developed for low Mach number two-phase flows applications. The use of a projection method to decouple pressure and velocity allows a greater time step than the one imposed by the acoustic CFL condition. Indeed, the acoustic terms are implicited during the pressure resolution. This formalism takes into account the local variation of density in both phase due to compressibility and with (or without) phase change. Besides, the Navier-Stokes equations are coupled with a CLSVOF method to ensure mass conservation and a

sharp description of the interface. The accuracy of the method is shown by comparing a reference solution with results obtained by compressible DNS in an oscillating water column configuration. Finally, the implementation of evaporation on a HIT configuration gives encouraging results that have to be pursued. Moreover, a 3D compressible simulation including more complex phenomena like collisions and breakups has been performed, showing the robustness of this formalism.

Acknowledgements

This work was granted access to the HPC resources of IDRIS, TGCC and CINES under the allocation A0032B06153 made by GENCI (Grand Equipement National de Calcul Intensif).

References

[1] B. Duret, G. Luret, J. Reveillon, T. Menard, A. Berlemont, and F.-X. Demoulin. DNS analysis of turbulent mixing in two-phase flows. *International Journal of Multiphase Flow*, 40(0):93 – 105, 2012.

[2] Sebastien Tanguy, Thibaut Menard, and Alain Berlemont. A Level Set Method for vaporizing two-phase flows. *Journal of Computational Physics*, 221(2):837 – 853, 2007.

[3] B. Duret, M. Al Qubeissi, C. Crua, and S. Sahzin. Evaporating droplets: comparisons between DNS and modelling. In *26th European Conference on Liquid Atomization and Spray Systems*, 2014.

[4] T. Menard, S. Tanguy, and A. Berlemont. Coupling level set/VOF/ghost fluid methods: Validation and application to 3d simulation of the primary break-up of a liquid jet. *International Journal of Multiphase Flow*, 33(5):510–524, May 2007.

[5] Sahadeb Kuila, T. Raja Sekhar, and D. Zeidan. A Robust and accurate Riemann solver for a compressible two-phase flow model. *Applied Mathematics and Computation*, 265(Supplement C):681–695, August 2015.

[6] Steven Schochet. The mathematical theory of low Mach number flows. *ESAIM: Mathematical Modelling and Numerical Analysis*, 39(3):441–458, May 2005.

[7] V. Daru, P. Le Quere, M. C. Duluc, and O. Le Maitre. A numerical method for the simulation of low Mach number liquid gas flows. *Journal of Computational Physics*, 229(23):8844–8867, November 2010.

[8] E. Knudsen, E. M. Doran, V. Mittal, J. Meng, and W. Spurlock. Compressible Eulerian needle-to-target large eddy simulations of a diesel fuel injector. *Proceedings of the Combustion Institute*, 36(2):2459–2466, January 2017.

[9] S. T. Miller, H. Jasak, D. A. Boger, E. G. Paterson, and A. Nedungadi. A pressure-based, compressible, two-phase flow finite volume method for underwater explosions. *Computers & Fluids*, 87(Supplement C):132–143, October 2013.

[10] Gregory Huber, Sebastien Tanguy, Jean-Christophe Bera, and Bruno Gilles. A time splitting projection scheme for compressible two-phase flows. Application to the interaction of bubbles with ultrasound waves. *Journal of Computational Physics*, 302(Supplement C):439–468, December 2015.

[11] Nipun Kwatra, Jonathan Su, Jon T. Gretarsson, and Ronald Fedkiw. A method for avoiding the acoustic time step restriction in compressible flow. *Journal of Computational Physics*, 228(11):4146–4161, June 2009.

[12] M. Boger, F. Jaegle, B. Weigand, and C. D. Munz. A pressure-based treatment for the direct numerical simulation of compressible multi-phase flow using multiple pressure variables. *Computers & Fluids*, 96(Supplement C):338–349, June 2014.

[13] M. Sussman, K. M. Smith, M. Y. Hussaini, M. Ohta, and R. Zhi-Wei. A sharp interface method for incompressible two-phase flows. *Journal of Computational Physics*, 221(2):469–505, February 2007.

[14] G. Vaudor, T. Menard, W. Aniszewski, M. Doring, and A. Berlemont. A consistent mass and momentum flux computation method for two phase flows. Application to atomization process. *Computers & Fluids*, 152(Supplement C):204–216, July 2017.

[15] Murray Rudman. A volume-tracking method for incompressible multifluid flows with large density variations. *International Journal for Numerical Methods in Fluids*, 28(2):357–378, August 1998.

[16] Myungjoo Kang, Ronald P. Fedkiw, and Xu-Dong Liu. A Boundary Condition Capturing Method for Multiphase Incompressible Flow. *Journal of Scientific Computing*, 15(3):323–360, September 2000.

[17] Samet Y. Kadioglu, Mark Sussman, Stanley Osher, Joseph P. Wright, and Myungjoo Kang. A second order primitive preconditioner for solving all speed multi-phase flows. *Journal of Computational Physics*, 209(2):477–503, November 2005.

[18] B. Koren, M. R. Lewis, E. H. van Brummelen, and B. van Leer. Riemann-Problem and Level-Set Approaches for Homentropic Two-Fluid Flow Computations. *Journal of Computational Physics*, 181(2):654–674, September 2002.